Deuterium depth distribution study in Yb[*]

Xing-Cai Guan(关兴彩)[1;1)]   Yong-Kai Lu(路咏凯)[1]   Hou-Jun He(何厚军)[1]   Jiang-Tao Zhao(赵江涛)[1]

Qiang Wang(王强)[1]   Kai-Hong Fang(方开洪)[1]   Xuan Meng(蒙萱)[1]   Tie-Shan Wang(王铁山)[1] Jirohta Kasagi[2]

[1]School of Nuclear Science and Technology, Lanzhou University, Tianshui South Road 222, Lanzhou, Gansu Province 730000, China
[2]Research Center for Electron Photon Science, Tohoku University, Sendai 980-8578, Japan

Abstract: The deuterium depth distribution for a 20 keV/D D_3^+ beam implanted into ytterbium (Yb) at a temperature between 300 and 340 K was studied using the D(d,p)T reaction. By analyzing the proton yields, the deuterium depth distribution from the front surface to 500 nm depth was found. The results indicate that an equilibrium deuterium distribution region from the front surface to a depth approximately equal to the mean range of implanted deuterons was formed in Yb during the implantation. The deduced deuterium concentration in the equilibrium deuterium distribution region was D/Yb = 22%.

1 Introduction

Measurements of hydrogen isotope depth profiles can provide information on the depth distribution of defects which are responsible for deposition and diffusion behaviors of hydrogen isotopes in materials and, therefore, can help to understand the mechanisms of the interactions between hydrogen isotopes and materials. Although many theoretical models have been developed to explain the diffusion behaviors of hydrogen isotopes in materials [1, 2], not enough experimental data, which are needed to study the physical processes governing the complicated behaviors of hydrogen isotopes in materials and verifying the models, have been observed because of experimental difficulties.

Since nuclear reactions can directly reflect information on the depth profiles of deuterium implanted into materials, the nuclear reaction analysis (NRA) technique is undoubtedly one of the possible techniques for observation of hydrogen isotope diffusion behaviors in materials. The NRA technique using the D(d, n)^{3}He or D(d, p)T reaction was proposed in the early 1970s to study deuterium depth profiles in materials [3, 4]. Thereafter, the NRA technique has been well developed and widely applied [5–14].

In this work, to study the deuterium depth distribution in metals, an ytterbium (Yb) foil was implanted by a high flux 20 keV/D D_3^+ beam at a temperature between 300 and 340 K. A 75 keV D^+ beam with lower flux

and fluence was employed to probe the deuterium depth distribution following the implantation and after about 66 hours. The proton yields of the D(d, p)T reaction for the implantation and probing beams were recorded during the experiment. The deuterium depth distribution from the front surface to 500 nm depth in Yb was obtained by analyzing these proton yields.

2 Experiment

The experiment was carried out using a low-energy high-current ion beam generator at the Research Center for Electron Photon Science, Tohoku University, Japan. The details of this ion beam generator have been described in [15, 16]. D^+, D_2^+ and D_3^+ beams can be extracted from the 25 kV duoplasmatron ion source of the experimental setup by using high-purity deuterium gas [17].

The experimental details of this work are similar to those given in [14, 18]. A high-purity (99.9%) Yb foil with a thickness of 75 μm was fixed horizontally on the target holder without heating or cooling. The target holder was placed at the center of a high vacuum (better than 3×10^{-5} Pa) target chamber. During the experiment, the deuterium ion beam bombarded the Yb target with an incident angle of 30° after passing through a diaphragm with a diameter of 8.5 mm. The beam spot area on the target was ~ 14 mm in diameter. A silicon

surface barrier detector (450 mm² in area and 300 μm in thickness) cooled by water was employed to detect the energies of the protons coming from the target with an exit angle of 50°. The distance from the detector center to the beam spot area center was ∼ 49 mm. The detector, which had a solid angle of ∼ 0.179 sr, was located at an angle of 125° with respect to the ion beam direction. A 50 μg/cm² thick carbon film was placed in front of the detector to prevent scattered deuterons from colliding with the detector directly.

During the experiment, the Yb foil was implanted by a 20 keV/D D_3^+ beam with a flux of 3.0×10^{14} D/cm²/s for ∼ 8.0×10^3 sec at a temperature between 300 and 340 K until it reached a saturation state, i.e., the recorded proton yields did not change with the accumulated implantation dose, as shown in Fig. 1.
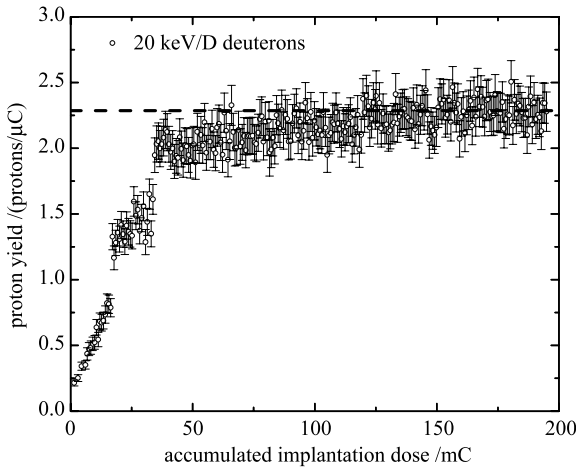

Fig. 1. Recorded proton yields of the D(d, p)T reaction for the implanted 20 keV/D D_3^+ beam as a function of accumulated implantation dose. The dashed line was drawn to guide the eye. The levelling-off of the proton yields following the initial rise signifies that a saturation state was reached.

Following the implantation, a D⁺ beam with an energy of 75 keV (the maximum energy of the beam provided by the ion beam generator used) and a current of 0.6 μA was applied to monitor the deuterium depth distribution in Yb foil, since the implanted deuterium concentration in the deeper region of the target was more accurately determined by a probing beam with higher energy. This probing beam was provided by the same experimental setup as the 20 keV/D D_3^+ implantation beam. The fluence of the probing beam was controlled so as not to cause noticeable unwanted changes in the deuterium concentration. In this step, the measured proton yield was (92.3 ± 2.0) protons/μC.

Then the Yb target was left in the high vacuum target chamber for about 66 h without any deuterium implantation. Thereafter, the deuterium depth distribution

was probed again by the 75 keV D⁺ beam and this time the measured proton yield was (92.4 ± 2.0) protons/μC, without any appreciable change compared to the proton yield measured 66 h previously. This indicates that the deuterium depth distribution showed no noticeable change over the 66 h period. Also, as expected, the employed probing beam did not induce conspicuous changes in the deuterium concentration.

The typical charged particle spectra obtained at E_d = 20 and 75 keV/D for the D(d, p)T reaction in Yb are shown in Fig. 2(a) and 2(b), respectively. Two peaks, which correspond to the tritons and protons emitted from the D(d, p)T reaction, are clearly observed in Fig. 2.
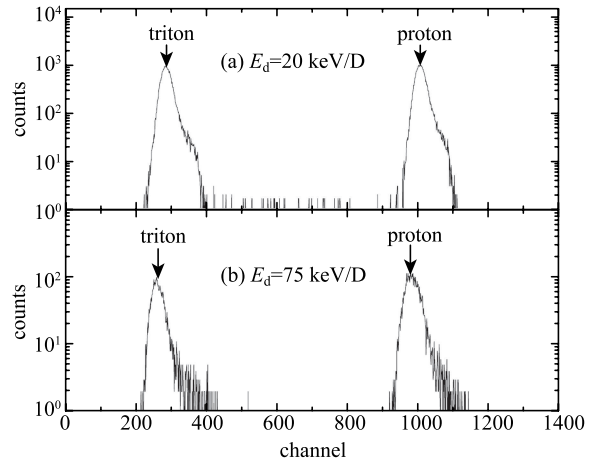

Fig. 2. Typical charged particle spectra for the D(d, p)T reaction in Yb obtained at E_d = (a) 20 and (b) 75 keV/D.

3 Analysis methods and results

The total proton yield $Y_p(E_0)$ of the D(d, p)T reaction in thick target can be expressed as [19, 20]

$$Y_p(E_0) = N_d \frac{\Omega_{lab}}{4\pi} \int_0^{E_0} N_D(x(E)) \frac{d\Omega_{cm}}{d\Omega_{lab}} \sigma(E) \left(\frac{dE}{dx}\right)^{-1} dE,$$
(1)

where E_0 is the incident energy, N_d is the number of incident deuterons, Ω_{lab} is the detector solid angle, $N_D(x(E))$ is the number of target deuterons (deuterium concentration), $d\Omega_{cm}/d\Omega_{lab}$ is the transformation coefficient of the solid angle between the center-of-mass (cm) system and the laboratory (lab) system, $\sigma(E)$ is the reaction cross section and dE/dx is the stopping power.

Taking into account the screening effect [21, 22], Eq. (1) can be transformed into

$$Y_{\mathrm{p}}(E_0) = N_{\mathrm{d}} \frac{\Omega_{\mathrm{lab}}}{4\pi} \int\limits_0^{E_0} N_{\mathrm{D}}\left(x\left(E\right)\right) \frac{\mathrm{d}\Omega_{\mathrm{cm}}}{\mathrm{d}\Omega_{\mathrm{lab}}}$$

$$\cdot f\left(E, U_{\mathrm{s}}\right) \sigma_{\mathrm{bare}}\left(E\right) \left(\frac{\mathrm{d}E}{\mathrm{d}x}\right)^{-1} \mathrm{d}E, \qquad (2)$$

where U_{s} is the constant screening energy provided by the environment where the reaction happens [23], $\sigma_{\mathrm{bare}}(E)$ is the reaction cross section for bare nuclei, $f(E, U_{\mathrm{s}}) \approx \exp(\pi\eta U_{\mathrm{s}}/E)$ is the enhancement factor [21], in which $\eta = Z_1 Z_2 \alpha (\mu c^2/E_{\mathrm{cm}})^{1/2}$ is the corresponding Sommerfeld parameter (Z_1 and Z_2 are atomic numbers of the target and projectile, α is the fine structure constant and μ is the reduced mass in amu).

For the D(d,p)T reaction in Yb, the U_{s} was estimated as 74.3 eV, including values of 20.4 eV estimated from the adiabatic limit due to the screening effect of bound electrons [24] and 71.4 eV calculated from the Thomas-Fermi Approximation because of the screening effect of conductive electrons [25]. Yuki et al. [19] studied the screening effect of the D(d, p)T reaction in Yb experimentally, and their deduced U_{s} was (81 ± 10) eV, in good agreement with the expected value used in this work.

In this work, the proton yield of the D(d, p)T reaction in Yb as a function of depth was calculated by a Monte-Carlo spectrum simulation program NRIBA code, whose details have been given in [14, 26]. The proton yields per unit deuterium concentration (D/Yb = 1%), $Y_{\mathrm{p}}(x_i)$, of the D(d,p)T reaction produced in a single layer (10 nm per layer) calculated by NRIBA code are shown in Fig. 3. Similar to what was done in Ref. [14], an effective reaction region, from which the proton yield is produced and which contributes $\sim 95\%$ to the total proton yield, was assumed in this work. The effective reaction regions were 0–130 and 0–500 nm for 20 and 75 keV/D deuterons, respectively.
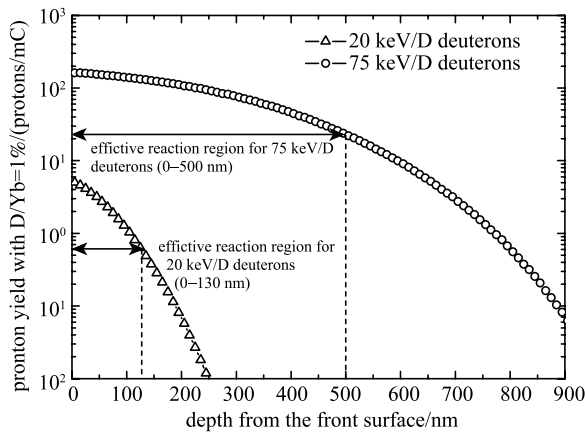

Fig. 3.   Proton yields with D/Yb = 1% produced in a single layer calculated by NRIBA code. The effective reaction regions were 0–130 and 0–500 nm for 20 and 75 keV/D deuterons, respectively.

Based on the view of Raiola et al. [27] that the deuterium depth distribution is nearly homogeneous within the region from the front surface to the mean range of implanted deuterons at saturation state, and similar to what was done in Ref. [14], it was assumed that the deuterium concentration N_{D} (D/Yb at.%) within the effective reaction region (0–130 nm) for 20 keV/D deuterons was uniform in this work. Thus, the proton yield $Y_{\mathrm{p}}(20)$ can be deduced from the following equation

$$0.95 Y_{\mathrm{p}}(20) = N_{\mathrm{D}} \sum_{i=1}^{13} Y_{\mathrm{p}}^{20}(x_i), \qquad (3)$$

where $Y_{\mathrm{p}}^{20}(x_i)$ is the proton yield per unit deuterium concentration produced in a single layer calculated by NRIBA code for 20 keV/D deuterons and $i = 1, 2, \cdots$ number of layers.

The deuterium concentration within the effective reaction region for 20 keV/D deuterons deduced from the experimental data is shown in Fig. 4. It shows that the deuterium concentration increases with the accumulated implantation dose until it reaches a saturation state after the dose reached ~ 120 mC. The linear fitting of the data after 120 mC resulted in D/Yb = $(22.3 \pm 0.7)\%$.
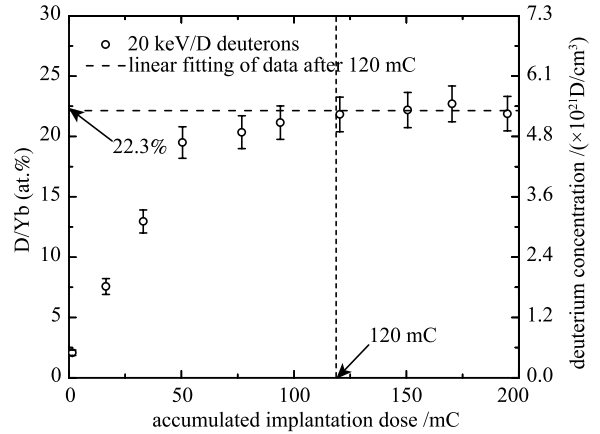

Fig. 4.   Deuterium concentration within the effective reaction region (0–130 nm) for 20 keV/D deuterons.   The deuterium concentration increases with the accumulated implantation dose until it reaches a saturation state.

The deuterium depth distribution for 20 keV/D deuterons implanted into Yb can also be obtained from simulation with SRIM [28] and the simulated result can be fitted by a quartic polynomial expressed as

$$N_{\mathrm{D}}(x) = a_0 + a_1 x + a_2 x^2 + a_3 x^3 + a_4 x^4, \qquad (4)$$

where $N_{\mathrm{D}}(x)$ is the deuterium concentration (unit: D/cm^3), a_0, a_1, a_2, a_3 and a_4 are parameters of the

quartic polynomial, and x is the depth beneath the front surface.

It is reasonable to assume that the deuterium concentration $N_D(x_i)$ in a single layer (10 nm per layer), which is derived from Eq. (4), is uniform. Thus, the total proton yield $Y_p(E_0)$ can be expressed as

$$Y_p(E_0) = \sum_{x=0}^{x} N_D(x_i) \cdot Y_p(x_i). \tag{5}$$

From Fig. 4, it is concluded that an equilibrium deuterium distribution was formed within the region from the front surface to at least 130 nm depth in Yb during the implantation after the accumulated implantation dose reached ~ 120 mC, while it was difficult to quantitatively determine the precise depth of the equilibrium deuterium distribution region. Thus, a parameter x_0, describing the depth of the equilibrium deuterium distribution region beneath the front surface, was used as an adjustable parameter in the data analysis process. So Eq. (5) can be transformed into

$$Y_p(E_0) = \left(A \cdot N_D(x_0) \sum_{x=0}^{x_0} Y_p(x_i) + \sum_{x=x_0}^{500} A \cdot N_D(x_i) \cdot Y_p(x_i) \right), \tag{6}$$

where $N_D(x_0)$ is the uniform deuterium concentration in the equilibrium deuterium distribution region (from the front surface to x_0) determined by the deuterium concentration at x_0, which can be deduced from Eq. (4), and A is an adjustable multiplication factor for the deuterium concentration.

Finally, the deuterium depth distribution from the front surface to 500 nm depth (effective reaction region for 75 keV/D deuterons) in Yb was obtained by varying the adjustable parameters x_0 and A together to fit the experimentally measured proton yields of the D(d, p)T reaction for the 20 keV/D D_3^+ implantation beam and the 75 keV D^+ probing beam, simultaneously. The resulting fit resulted in fitting proton yields of $Y_p'(20) = 2.28$ protons/μC and $Y_p'(75) = 92.4$ protons/μC, which agree well with the experimental data with values of (2.28 $\pm$ 0.05) and (92.3 $\pm$ 2.0) protons/μC for the 20 keV/D D_3^+ and 75 keV D^+ beams, respectively. The obtained deuterium depth distribution is shown in Fig. 5.

4   Discussion

Since the fitting proton yields calculated by Eq. (6) coincide well with the experimental data, it is concluded that the present result shown in Fig. 5 can quantitatively characterize the deuterium depth distribution in Yb.

From Fig. 5, it is found that an equilibrium deuterium distribution region from the front surface to ~ 260 nm depth was formed in Yb during the implantation. According to the simulated result from SRIM [28],

the mean range of 20 keV/D deuterons in Yb is about 250 nm, which agrees well with the depth of the formed equilibrium deuterium distribution region. The deuterium concentrations in the equilibrium deuterium distribution region at a temperature between 300 and 340 K deduced from Eqs. (3) and (6) are consistent with each other, while they are higher than the deuterium concentration (D/Yb = 13%) at a temperature of 473 K and significantly lower than the deuterium concentration (D/Yb = 130%) at room temperature obtained by Raiola [29]. It should be mentioned that Zhao et al. [14] studied the dynamic saturated deuterium concentration in beryllium by the D(d, p)T reaction at a temperature between 300 and 340 K, and their obtained saturated D/Be was about 20%, in agreement with the value of D/Yb obtained in this work.
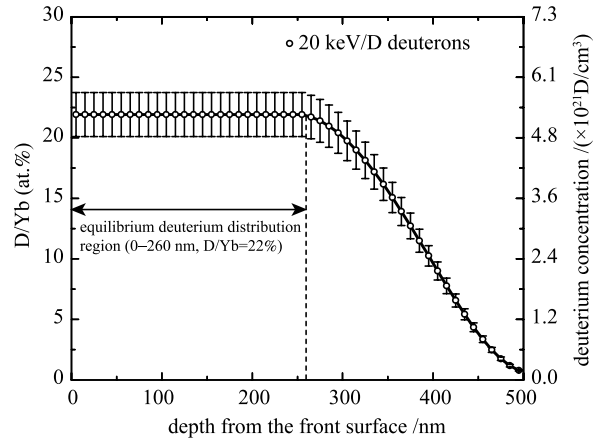

Fig. 5.   Deuterium depth distribution for 20 keV/D deuterons implanted into Yb foil. An equilibrium deuterium distribution region from the front surface to ~ 260 nm depth with D/Yb = 22% was formed.

As mentioned in Section 2, the deuterium depth distribution showed no appreciable change over a 66 h period after the implantation. Furthermore, the presence of a certain deuterium concentration near the front surface in Yb suggested that considerable deuterium diffusion occurred during the implantation. A similar phenomenon was also observed by Lewis when he studied deuterium migration and tripping in uranium [30], and the irradiation enhanced diffusion phenomenon during ion irradiation [31] was employed to explain his results. However, ion-induced defects and dislocations usually create defect densities of a few % at maximum, but not the very high deuterium trap density up to $\sim 22\%$ obtained in this work. Since the deuterons deposited in metals were in the form of separated atoms and D_2 molecules, which have been confirmed in beryllium [32], such high deuterium concentration might be caused by the implanted deuterons being precipitated into gas bubbles formed in the target during the implantation.

5   Conclusions

In this work, an Yb foil, implanted by a high flux 20 keV/D D_3^+ beam at a temperature between 300 and 340 K, was employed to study the deuterium depth distribution in metals. A 75 keV D^+ beam with lower flux and fluence was used to probe the deuterium depth distribution following the implantation and after about 66 h.

By analyzing the proton yields of the D(d, p)T reaction for the implantation and probing beams, the deuterium depth distribution from the front surface to 500 nm depth in Yb was found in this work. The present results showed that an equilibrium deuterium distribu-tion was formed in Yb within the region from the front surface to a depth of $\sim$ 260 nm, which is approximately equal to the mean range of implanted 20 keV/D deuteron in Yb. The deduced deuterium concentration (D/Yb) in the equilibrium deuterium distribution region was $\sim$ 22%.

The relevant work is still going on to accumulate more especially necessary data for studying the phys-ical processes governing the complicated behaviors of deuterium in metals, such as tungsten, molybdenum, beryllium, samarium, palladium and gold.

References

1   P. G. Shewmon, *Diffusion in solids* (New York: McGraw-Hill, 1963)
2   J. R. Manning, *Diffusion kinetics for atoms in crystals* (New York: D.V. Nostrand, 1968)
3   C. M. Bartle et al, Nucl. Instrum Methods, **95**: 221–228 (1971)
4   P. B. Johnson, Nucl. Instrum Methods, **114**: 467–475 (1974)
5   A. E. Pontau et al, J. Nucl. Mater., **91**: 343–346 (1980)
6   Y. Takeuchi et al, J. Appl. Phys., **64**: 2959–2963 (1988)
7   S. M. Myers et al, Phys. Rev. B, **43**: 9503–9510 (1991)
8   H. Kudo et al, J. Nucl. Mater., **258−263**: 622–627 (1998)
9   Z. Qin et al, J. Nucl. Mater., **264**: 228–233 (1999)
10 N. Kawachi et al, Nucl. Instrum Methods B, **190**: 195–198 (2002)
11 V. Kh. Alimov et al, J. Nucl. Mater., **337−339**: 619–623 (2005)
12 D. J. Cherniak et al, Chem. Geol., **268**(1): 155-166 (2009)
13 W. R. Wampler et al, J. Nucl. Mater., **415**(1): S653–656 (2011)
14 J.T. Zhao et al, Nucl. Instrum. Methods B, **316**: 13–16 (2013)
15 H. Yuki et al, J. Phys. Soc. Jpn., **66**: 73–78 (1997)
16 K. H. Fang et al, J. Phys. Soc. Jpn., **80**: 084201 (2011)
17 J. T. Zhao, Ph. D. thesis (Lanzhou University, 2013)
18 J. T. Zhao et al, Nucl. Instrum Methods B, **299**: 54–60 (2013)
19 H. Yuki et al, J. Phys. G: Nucl. Part. Phys., **23**: 1459–1464 (1997)
20 H. Y. Lv et al, Chinese Phys. C, **35**: 26–30 (2011)
21 H. J. Assenbaum et al, Z. Phys. A, **327**: 461–468 (1987)
22 S. Engstler et al, Phys. Lett. B, **202**: 179–184 (1988)
23 T. S. Wang et al, J. Phys. G: Nucl. Part. Phys., **39**: 015201 (2012)
24 L. Bracci et al, Nucl. Phys. A, **513**: 316–343 (1990)
25 C. Kittel, *Introduction to Solid State Physics* (New York: John Wiley & Sons, Inc., 1986)
26 T. S. Wang et al, Nucl. Instrum Methods B, **269**: 2721–2725 (2011)
27 F. Raiola et al, Eur. Phys. J. A, **13**: 377–382 (2002)
28 J. F. Ziegler, J. P. Biersack, *code SRIM* (http://www.srim.org)
29 F. Raiola, Ph. D. thesis (Ruhr-Universität Bochum, 2005)
30 M. B. Lewis, J. Nucl. Mater., **88**: 23–30 (1980)
31 S. T. Picraux, F. L. Vook, Radiation Effects, **11**: 179–192 (1971)
32 V. Kh. Alimov et al, J. Nucl. Mater., **241−243**: 1047–1052 (1997)